Controlled growth of aluminum oxide thin films on hydrogen terminated Si(0 0 1) surface

S. Vizzini[a,*], H. Oughaddou[a], C. Léandri[a], V.K. Lazarov[b], A. Kohn[b], K. Nguyen[a],
C. Coudreau[a], J.-P. Bibérian[a], B. Ealet[a], J.-L. Lazzari[a], F. Arnaud d'Avitaya[a], B. Aufray[a]

[a]CRMN-UPR-CNRS 7251, Case 913, 13288 Marseille cedex 09, France
[b]Department of Materials, University of Oxford, Parks Road, Oxford OX1 3PH, UK

Abstract

Auger electron spectroscopy, energy electron loss spectroscopy, atomic force microscopy and transmission electron microscopy were used to characterize ultra-thin aluminum oxide films grown on hydrogen-terminated Si(0 0 1)–H substrates via a specific atomic layer deposition and oxidation technique. Oxide thin films grown in such a way are highly stable with temperature at least up to 700 °C. Band gap was estimated to be 6.6 ± 0.2 eV, independent of thickness. Formation of the oxide layer slightly increases the initial roughness of silicon surface. Furthermore, no silicon oxide was found at the aluminum oxide–silicon interface.

1. Introduction

Aluminum oxide has been extensively studied in recent years mainly for its technological applications in catalysis [1] and as an insulating barrier in magnetic tunnel junctions [2]. In all cases, and especially for magnetic tunnel junctions, control growth of ultra-thin oxide films is of crucial importance. Many studies were performed to determine most accurate processes and best experimental conditions to grow well-defined and homogeneous oxide layers [3–6].

Previously, using a specific atomic layer deposition and oxidation (ALDO) procedure, we studied growth of ultra-thin aluminum oxide films on a metallic substrate: Ag(1 1 1) [7]. The ALDO procedure described in Ref. [7] is a repetition of the following steps: (i) evaporation at room temperature (RT) of one aluminum monolayer (1 Al ML),

(ii) oxidation at RT ($\sim 10^{-6}$ Torr of molecular oxygen for 5 min) and (iii) annealing at intermediate temperatures (400 °C) under-ultra high vacuum (UHV) conditions. We showed by Auger electron spectroscopy (AES) that the oxidation process of the first deposited aluminum monolayer was fast, complete and self-limited to the topmost aluminum monolayer. Furthermore, these oxides are highly stable with temperature since there is no concentration and structure changes upon annealing at 500 °C under UHV conditions.

Using the same ALDO procedure, we report in this paper chemical composition, atomic structure, band gap, and roughness of aluminum oxide thin films grown on hydrogen-terminated Si(0 0 1) substrates (Si(0 0 1)–H). Due to the important technological applications of these thin oxide layers in magnetic tunnel junctions, we also report atomic structure and roughness of Co/AlO/Si(0 0 1) stacks.

Furthermore, we used Si(1 0 0) hydrogen terminated in order to avoid silicon oxide at the surface which could affect the spin–injection process into this substrate.

*Corresponding author. Fax: +33 4 91 82 91 97.
E-mail address: vizzini@crmcn.univ-mrs.fr (S. Vizzini).

2. Results and discussion

The substrate preparation consist of a 50 s dip treatment of the Si(0 0 1) surface in 10% HF-deionized water-diluted solution followed by rinsing in water in order to get a Si(0 0 1) surface hydrogen terminated.

After the chemical treatment, the samples were immediately introduced in the UHV chamber and surface cleanliness were checked by AES. Aluminum was deposited in the UHV chamber in the low 10^{-9} Torr background pressure range with a deposition rate of about 0.5 ML/min (calibration was performed previously using a quartz micro-balance and Auger spectroscopy [7]). The oxidation process is performed at RT in the same chamber after isolation of the aluminum source by an UHV lock-valve. Oxidation was performed under molecular oxygen pressure of 2×10^{-6} Torr for 5 min.

Fig. 1 shows the AES spectra corresponding to the clean Si(0 0 1)–H surface, then after deposition of 1 Al ML and finally after oxidation as described above.

As observed with the Ag(1 1 1) substrate [7], the 68 eV Auger peak characteristic of pure aluminum is shifted to 56 eV after the oxidation and an oxygen Auger peak (at 511 eV) appears. Furthermore, these Auger spectra do not change with oxygen exposure time which indicates that the oxidation process is also very rapid on this substrate. Using attenuations of the Si Auger intensity peak (52% after the deposition of 1 Al ML and of 32% more after the oxidation process), we calculated the thickness of the first oxide layer: 0.7 ± 0.2 nm. This value is very close to the one determined on Ag(1 1 1) (0.8 nm) [7].

In order to check thermodynamic stability of this superficial oxide (Al_xO_y) grown at RT, we annealed the sample up to 700 °C for 30 min under UHV conditions. This thermal treatment does not affect the superficial oxide since we do not observe any evolution or modification of the various Auger peaks in relative intensities as well as in

energy position. This absence of dissolution or evaporation of aluminum and/or oxygen atoms at elevated temperature clearly shows a large thermal stability of this superficial oxide. The oxidation process stabilizes the aluminum atoms at the surface forming a stable Al_xO_y artificial compound. As shown in Fig. 1, there is no shift of the silicon Auger peak, indicating that the oxidation process is limited to the aluminum layer even after annealing at high temperature.

After three cycles of deposition–oxidation of 1 Al ML, the Si Auger peak disappears, completely screened by the superficial oxide as shown on the spectrum of Fig. 2. Assuming that oxygen and aluminum atoms are randomly distributed in the oxide layer and that there is no composition variation in the topmost surface layer, we calculated the approximate composition of the oxide Al_xO_y, using elementary Auger sensitivity factors $S_{Al} = 0.25$ and $S_O = 0.5$ for aluminum and oxygen [8].

Atomic fractions X_i for each element are calculated applying the relation:

$$X_i = \frac{I_i}{S_i} \left(\sum_i \frac{I_i}{S_i} \right)^{-1},$$

where I_i is the peak-to-peak intensity Auger signal of element i. From the intensities measured on the spectrum of Fig. 2, we obtain chemical composition very close to AlO. This specific chemical composition is probably linked to the ALDO procedure used here. Indeed this method, which is based on a self-limitation of the oxidation process via a chemical-adsorption phenomenon, determines a chemical composition which can be different from the expected Al_2O_3 composition. Furthermore, sample annealing being performed under UHV conditions, i.e. at very low partial pressure of oxygen, the chemical composition of the aluminum oxide cannot change during this process.
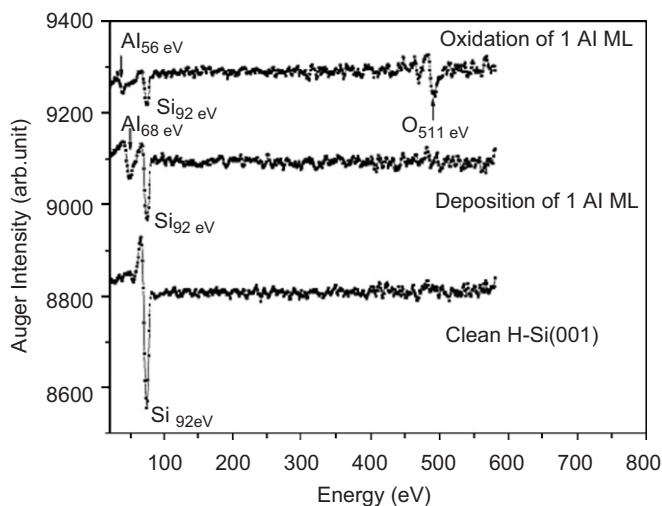

Fig. 1. AES spectra corresponding to the clean Si(0 0 1)–H surface, after deposition of 1 Al ML and after the oxidation process of this first Al ML.
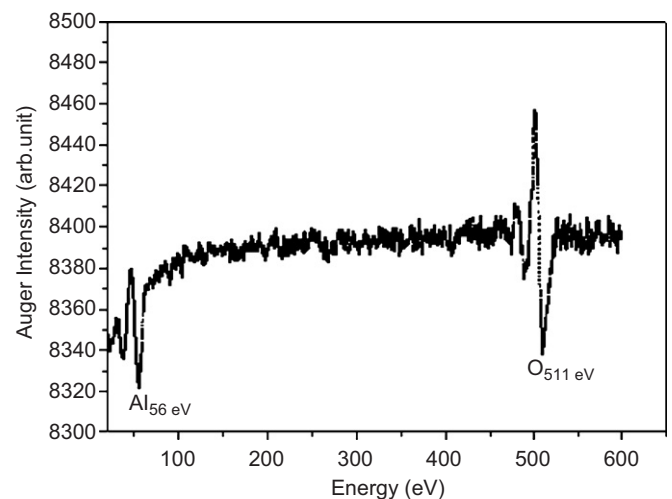

Fig. 2. AES spectrum recorded after three runs of deposition/oxidation of 1 Al ML.
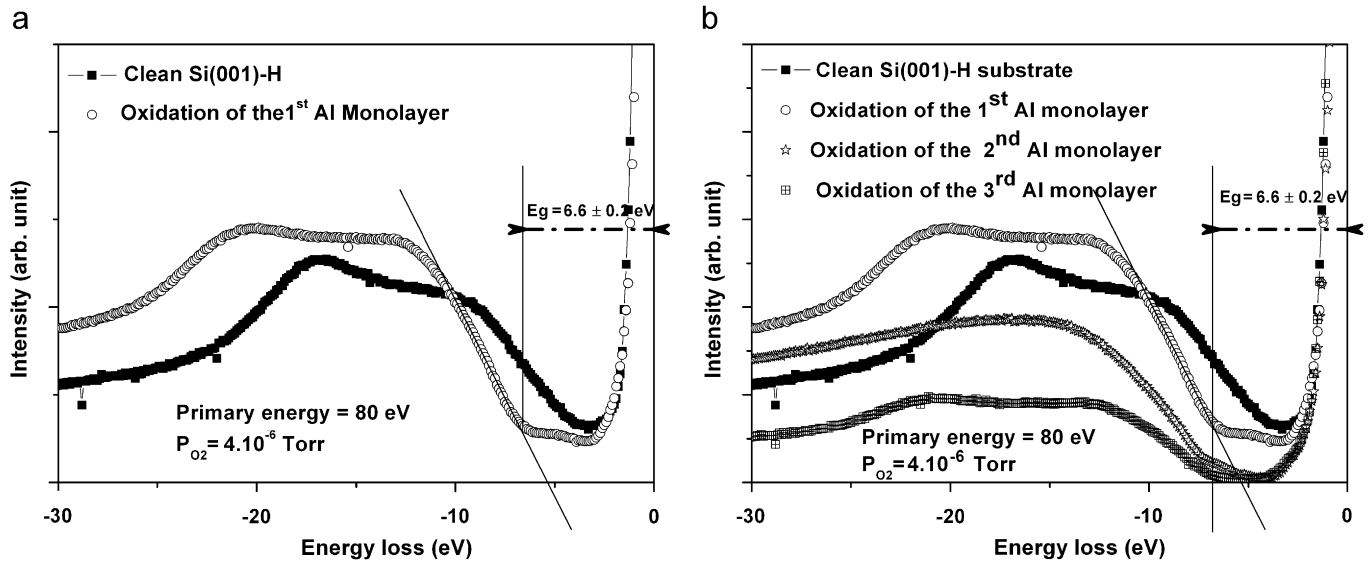
Fig. 3. EELS spectra (a) on Si(0 0 1)–H surface, then after the first oxidation process (b) same as (a), but with two and three oxide layers.

Band gap of the oxide layer is measured using energy electron loss spectroscopy (EELS). Fig. 3a shows EELS spectra recorded on clean Si(0 0 1)–H surface, then after the oxidation process of 1 Al ML. The band gap of the oxidized layer was estimated to 6.6 ± 0.2 eV using a method described in Ref. [2].

Fig. 3b shows the evolution of the EELS spectra versus oxide thickness, i.e. from clean surface to three deposition–oxidation cycles. The band gap does not change with thickness within experimental errors.

On Si(0 0 1)–H substrate, we grew an oxide layer (AlO) corresponding to three ALDO cycles then on top of this oxide layer, we deposited in situ by molecular beam epitaxy (MBE) a 50-nm-thick cobalt layer. The choice of cobalt, which is a typical ferromagnetic material, is related to its large use in magnetic tunnel junctions. This device was characterized using high-resolution and analytical transmission electron microscopy (HR-TEM). Cross-sectional specimens were prepared by mechanical thinning and polishing. Then, the specimens were made electron transparent by low angle and low-energy ion milling.

Fig. 4 shows bright field (BF) images of a Co/AlO/Si cross-section sample, where the Si substrate is approximately oriented along the Si$\langle 0\,1\,1 \rangle$ zone axis. At this magnification, the polycrystalline cobalt film appears continuous and uniform in thickness with a surface roughness of about 4 nm. An HR-TEM image (Fig. 5) shows more precisely the atomic structure of the silicon substrate (atomic columns of silicon are visible). On this image, the oxide layer appears amorphous as confirmed by convergent beam electron diffractions. The oxide is continuous on the Si substrate, with no apparent pinholes. The thickness of this Al oxide is approximately 2.1 nm, which is in good agreement with the previous calculations based on the attenuation of the silicon Auger peak (3×0.7 nm = 2.1 nm). The interface between the silicon
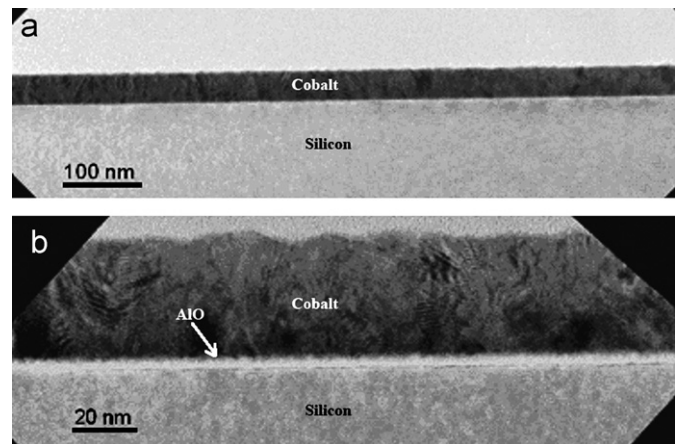

Fig. 4. BF-TEM images from a cross-section of Co/AlO/Si structures at different magnifications. The Si substrate has been oriented to the [1 1 0] zone axis.

substrate and the oxide layer is atomically sharp with a roughness of 0.4 nm.

We would like to stress that the transmission electron microscopy (TEM) does not give an accurate measurement of the roughness because we see a 2D projection of the sample. Consequently, we may underestimate this roughness parameter as compared with the atomic force microscopy (AFM) measurements.

In order to confirm this local roughness values measured by TEM at both interfaces AlO/Si and Co/AlO, a systematic study by ex situ AFM in non-contact mode is performed.

Fig. 6a shows a typical AFM image recorded after the oxidation of 1 Al ML deposited on a Si(0 0 1)–H surface. The surface roughness of the deposited oxide is small (RMS = 0.4), which suggests that aluminum wets perfectly the Si(0 0 1)–H surface without islands formation as locally observed by TEM.
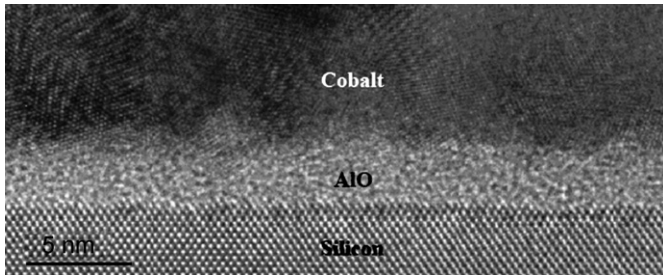
Fig. 5. HR-TEM images of a Co/AlO/Si stack. The Si substrate is oriented along the [1 1 0] zone axis.
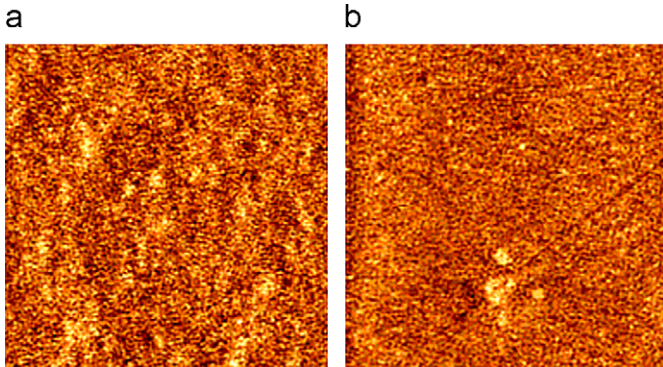

Fig. 6. AFM images recorded in non-contact mode ($5\,\mu m^2$): (a) after growth of one AlO layer on Si(0 0 1)–H (RMS = 0.42 nm) and (b) after growth of three AlO layers (RMS = 0.61 nm).

Fig. 6b shows AFM image after three ALDO cycles. The surface roughness value (RMS = 0.6 nm) is close to the one measured after one run (RMS = 0.4 nm). Therefore, as seen locally by TEM, the aluminum oxide grown using this process does not add any excess of roughness which also means that the oxide grows indeed layer by layer. The surface of the oxide remained very smooth during the whole growth. The surface roughness does not exceed 0.7 nm after five ALDO cycles.

3. Conclusion

The specific atomic layer deposition and oxidation procedure, i.e. a repetition of the following steps: (i) 1 Al ML deposition, (ii) oxidation at RT and (iii) annealing in UHV conditions, allows very precise control of the growth of a superficial aluminum oxide on Si(0 0 1)–H. By AES, EELS, HR-TEM, and AFM, we demonstrated that this oxide is amorphous, homogeneous throughout the whole thickness of the oxide layer and with a chemical composition close to AlO. The oxide is stable up to $700\,^{\circ}C$ and exhibits a band gap of $6.6 \pm 0.2\,eV$. We also show that this process allows growth of metal insulator semiconductor (MIS) structures with abrupt interfaces at the atomic scale. These results are very promising for achieving MTJ structures directly on Si with excellent growth control.

References

[1] H.J. Freund, E. Umbach, Adsorption of Ordered Surfaces of Ionic Solids and Thin films, Springer, Heidelberg, 1993.
[2] J.S. Moodera, L.R. Kinder, J. Appl. Phys. 79 (1996) 4724.
[3] S.A. Chambers, Surf. Sci. Rep. 39 (2000) 105.
[4] R. Franchy, Surf. Sci. Rep. 38 (2000) 195.
[5] J.H. Park, G.S. Lee, J.Y. Yang, K.S. Yoon, C.O. Kim, J.P. Hong, H. Kim, J. Appl. Phys. Lett. 80 (21) (2002) 3982.
[6] V. Rose, V. Podgursky, I. Costina, R. Franchy, Surf. Sci. 541 (2003) 128.
[7] H. Oughaddou, S. Vizzini, B. Aufray, B. Ealet, J.-M. Gay, J.-P. Bibérian, F. Arnaud D'Avitaya, Appl. Surf. Sci. 252 (2006) 4167.
[8] Lawrence E. David, et al, Handbook of Auger Electron Spectroscopy, second ed., Physical Electronics Industries, Inc.